Second backbend in the mass $A \sim 180$ region

A. Ansari
Institute of Physics, College of Arts and Sciences, University of Tokyo, Komaba, Meguro-ku, Tokyo 153-8902, Japan
and Institute of Physics, Bhubaneswar - 751 005, India
(Received 18 September 1998)

Within the framework of self-consistent cranked Hartree-Fock-Bogoliubov theory (one dimensional) we predict a second backbend in the yrast line of ^{182}Os at $I \approx 40\hbar$, which is even sharper than the first one observed experimentally at $I \approx 14\hbar$. Around such a high spin the structure becomes multiquasiparticle type, but the main source of this strong discontinuity is a sudden large alignment of $i_{13/2}$ proton orbitals along the rotation axis followed soon by the alignment of $j_{15/2}$ neutron orbitals. This leads to drastic structural changes at such high spins. When experimentally confirmed, this will be observed for the first time in this mass region, and will be at the highest spin so far. [S0556-2813(99)05505-3]

PACS number(s): 21.60.Jz, 21.10.Re, 21.60.Ev, 27.70.+q

During the latter half of the 1970s and early 1980s when research activities in high spin spectroscopy were rather at their peak, experimentally as well as theoretically, it was the one-dimensional cranking [rotation about a principal axis (x) perpendicular to the symmetry axis (z)] Hartree-Fock-Bogoliubov (CHFB) theory [1–7] which was most successful (besides its well-known shortcomings) to explain the underlying mechanism of the backbending features observed in the moment of inertia (or spin) versus rotational frequency plot of the yrast levels (level with the lowest energy for a given angular momentum). This is because of the fact that the mechanism of the alignment of single-particle angular momenta along the rotation axis (the effect of collective rotation on single-particle motion) is naturally present in this approach.

After exhaustive activities in the rare-earth region, now the high-spin structure work has spread to all the mass regions of the periodic table with the maximum spin value reached being of the order of $I = 50\hbar$ (it is $60\hbar$ for the first superdeformed band in ^{152}Dy). Besides the yrast sequence, several sidebands are observed in most of the nuclei. Recently very interesting features have been observed in some of the nuclei near the upper end of the rare-earth region, namely, in W-Os isotopes with mass number $A \sim 180$ [8–13]. In some even-even isotopes sidebands are found with high-K band heads (K being the projection of I along the z axis) very close to the yrast line with signature [$r = (-1)^I$] symmetry broken; that is, even- and odd-spin states are connected by $B(M1)$ transitions and the ratio $B(M1)/B(E2)$ is found to be large. Such states with mixed signature symmetry are interpreted as t bands [14] arising due to the rotation of the nucleus about an axis tilted with respect to the principal axes of the quadrupole-shaped deformed nucleus. Some of the states of these high-K bands decay to the yrast states, particularly in the band crossing region. So it becomes natural to expect that the mutual interaction between these unperturbed bands should influence the backbending behavior in the yrast sequence. Also in this mass region the Fermi surface lies in the high-m states of high-j orbitals (e.g., $0h_{11/2}$ for protons and $0i_{13/2}$ for neutrons) which also gives some credence to such expectation that the yrast states, at least in the band crossing region, could be generated by tilted axis rotation. Thus, it has become an interesting and challenging problem to test if the usual explaination of backbending caused by the crossing of the s band (low-m $i_{13/2}$ neutron-aligned band) still holds. This question is not yet resolved through a microscopic quantal many-body calculation. It may be added that currently Onishi and his collaborators [15,16] are attempting to perform a generator coordinate method (GCM) calculation for ^{182}Os treating the tilting angles as generator coordinates. The good angular-momentum-projected GCM wave functions would be able to elucidate on the distribution of K components for a given value of the angular momentum.

In some odd-A nuclei in this mass region it has recently been found that the high-K bands really cross the ground band, producing backbend in the yrast sequence, e.g., ^{179}W [11] and ^{181}Re [12]. However, for even-even nuclei the general conclusion so far is that it is still the normal s-band crossing that plays an essential role in producing the backbend in these nuclei [9]. Furthermore, in a recent microscopic theoreical analysis of the tilted axis rotation following the band-mixing spin-projected shell model approach [17] it is found that in the case of ^{178,180,182}W and ^{184}Os the backbend originates due to normal s-band crossing; the tilted bands appear slightly above the yrast line. In view of these findings we thought of checking as to how the traditional CHFB approach works for this mass region. Particularly for very high spins $I > 20\hbar$, the usual CHFB theory is expected to work well, and angular momentum projection is almost impracticable. Hence, we have carried out here a self-consistent CHFB calculation for ^{182}Os in an appropriate single-particle model space. For this nucleus presently the yrast line extends up to $I = 34\hbar$ [8,13] without a second backbend and the calculation has been performed for spins up to $I = 50\hbar$. We find a strong backbend at around $I = 40\hbar$. In the following we present our results and discussions on these. Also from now on the spin values will be understood to be in units of $\hbar$.

Since the CHFB theory [2,4] is well known, we will not give any details here. For the Hamiltonian of the system we have used a pairing-plus-quadrupole model interaction. However, in addition, a hexadecapole term is also considered as these nuclei are expected to have large (negative) hexade-

TABLE I. Intrinsic shape parameters as a function of spin I [actually $\sqrt{I(I+1)}$]. For the ground state $\gamma=0$ and β, β_4, Δ_p, and Δ_n are, respectively 0.228, -0.038, 0.871 MeV, and 0.879 MeV in case ''Q4'' and 0.229, 0.0, 0.872 MeV, and 0.886 MeV in case ''Q2.'' At $I=10$, $\Delta_n=0.436$ MeV in the former case and 0.432 MeV in the latter case. It goes to zero for $I\geqslant 14$.

	With hexadecapole				Without hexadecapole		
I		γ		Δ_p		γ	Δ_p
($\hbar$)	β	(deg)	β_4	(MeV)	β	(deg)	(MeV)
0	0.228	0.0	-0.038	0.871	0.229	0.0	0.872
10	0.235	1.58	-0.039	0.799	0.237	1.35	0.796
20	0.224	5.89	-0.047	0.699	0.227	4.11	0.571
30	0.207	10.58	-0.050	0.0	0.208	9.53	0.0
38	0.217	0.97	-0.050	0.0	0.203	8.62	0.262
40	0.253	-11.11	-0.025	0.0	0.209	4.88	0.230
42	0.256	-12.80	-0.020	0.0	0.260	-12.52	0.0
50	0.245	-12.70	-0.021	0.0	0.253	-12.63	0.0

capole deformation β_4 [18]. The total Hamiltonian can be written as

$$\hat{H}=\hat{H}_0-\frac{1}{2}\sum_{\lambda=2,4}\chi_\lambda\sum_\mu \hat{Q}_{\lambda\mu}(-1)^\mu\hat{Q}_{\lambda-\mu}$$

$$-\frac{1}{4}\sum_{\tau=p,n}G_\tau\hat{P}^\dagger_\tau\hat{P}_\tau, \tag{1}$$

where χ_λ and G_τ are the corresponding interaction strengths (in MeV), and the multipole moments ($\hat{Q}_{\lambda\mu}$) and the pairing operator ($\hat{P}$) have standard forms [2], the radial part of the former being (r^2/b^2), with b as the oscillator length parameter. $\hat{H}_0$ represents the spherical part of the Hamiltonian with the single-particle (s.p.) orbitals (assuming $Z=40$, $N=70$ core) $2s_{1/2}$, $1d_{3/2}$, $1d_{5/2}$, $0g_{7/2}$, $0g_{9/2}$, $0i_{13/2}$, $1f_{7/2}$, $0h_{9/2}$, and $0h_{11/2}$ for protons and $2p_{1/2}$, $2p_{3/2}$, $1f_{5/2}$, $1f_{7/2}$, $0h_{9/2}$, $0h_{11/2}$, $0j_{15/2}$, $1g_{9/2}$, $0i_{11/2}$, and $0i_{13/2}$ for neutrons. The s.p. energies are as given in Table I of Ref. [15] except that of $0j_{15/2}$ which is 7.179 MeV. These energies are essentially the Nilsson spherical s.p. energies for this mass region.

As indicated above, Eq. (1) actually represents two Hamiltonians as far as numerical calculations are concerned here. One is as it is, and in the other the hexadecapole term is dropped. Correspondingly we have two sets of ineraction strengths which can reproduce more or less the ground state intrinsic shape parameters of ^{182}Os. Finally taking the principal x axis as the cranking axis the CHFB eigenvalue equations are solved by diagonalization with the usual particle number and angular momentum constraints [2,4].

We have also computed rotational g factors using the standard cranking expression [6]

$$g_I=\langle\hat{\mu}_x\rangle/\sqrt{I(I+1)}, \tag{2}$$

where $\hat{\mu}_x$ is the x component of the magnetic moment operator,

$$\hat{\mu}=g_l\sum_i \hat{j}_x(i)+(g_s-g_l)\sum_i \hat{s}_x(i), \tag{3}$$

with $g_l=1$ and $g_s=5.586$ for protons and $g_l=0$ and $g_s=-3.826$ for neutrons. In numerical computation the values of g_s are attenuated by a factor of 0.6 [6,11].

The CHFB equations are solved self-consistently in terms of seven collective variables when the hexadecapole (Q4) term is also present in the Hamiltonian. These are the pairing gaps Δ_p and Δ_n for protons and neutrons, respectively, and deformation parameters $q_{\lambda\mu}=q_{\lambda-\mu}=\langle\hat{Q}_{\lambda\mu}\rangle$, with $\mu=0,2$ for $\lambda=2$ and $\mu=0,2,4$ for $\lambda=4$. The usual deformation parameters (β,γ) and β_4 are defined through the relations $\hbar\omega_0\beta\cos\gamma=\chi_2 q_{20}$, $\hbar\omega_0\sin\gamma/\sqrt{2}=\chi_2 q_{22}$, and $\hbar\omega_0\beta_4=\chi_4 q_{40}$, where $\hbar\omega_0=41/A^{1/3}$ MeV.

When only the quadrupole interaction is considered then the degree of freedom is reduced to 4. As already mentioned, the interaction strengths are chosen such that the values of the ground state shape parameters (see Table I) are approximately reproduced [8,18]. The values of the pairing gap parameters are decided by looking at the experimental odd-even mass differences. It may be emphasized that after fixing the interaction strength parameters at this stage there are no free parameters in the theory. In the following, for the sake of brevity, when both quadrupole + hexadecapole interaction terms are considered, then the corresponding results will be indicated by the symbol ''Q4.'' But if only the quadrupole term is considered, then it will accordingly be indicated by ''Q2.''

Now we can discuss some of our main results. In Table I we have listed the values of the shape parameters at a few angular momentum values, the dependence on I being most striking around $I=40$. In both the cases, with and without the Q4 term, Δ_n goes to zero at $I=14$. On the other hand Δ_p vanishes at $I=30$ in the presence of the Q4 term and at $I=26$ without it, which implies a somewhat stronger proton pairing correlation in the former case for the spin range of about $I=16$–28. We find that when only quadrupole force is considered the proton pairing recovers for $I=34$ ($\Delta_p=0.214$ MeV) to $I=40$ ($\Delta_p=0.239$ MeV). In the other case it recovers only at one spin, $I=34$, with a small value of $\Delta_p=0.174$ MeV. In both the cases there is a correlation between γ acquiring a negative value and an increase in the value of β. Around spin $I=40$, γ changes sign from positive to negative by a quite sizable amount, and associated with it the value of β increases by about 20% (stretching). At the same time the value of β_4 shows a sudden decrease. However, it may be pointed out that now all the three components of $q_{4\mu}$, $\mu=0,2,4$, become of similar magnitude: for instance, at $I=38$ these are -8.05, -1.09, and 1.08 which become -4.10, -2.36, and 2.56 (all in units of b^2) at $I=40$ for $\mu=0$, 2, and 4, respectively.

In Fig. 1 we display a backbending (BB) plot of spin versus rotational frequency (ω) where for the experimental case $\omega_I=\frac{1}{2}(E_I-E_{I-2})$. As indicated on the top right corner of the figure, the three curves correspond to the experimental data, with hexadecapole (Q4) and without hexadecapole (Q2) terms in the Hamiltonian of Eq. (1). We notice that the first backbend is actually not well reproduced, though an upbend is produced at more or less the correct frequency, and the inclusion of the hexadecapole degrees of freedom helps in the right direction. However, the alignment of $0i_{13/2}$ neutron orbitals is quite pronounced as can be seen in the

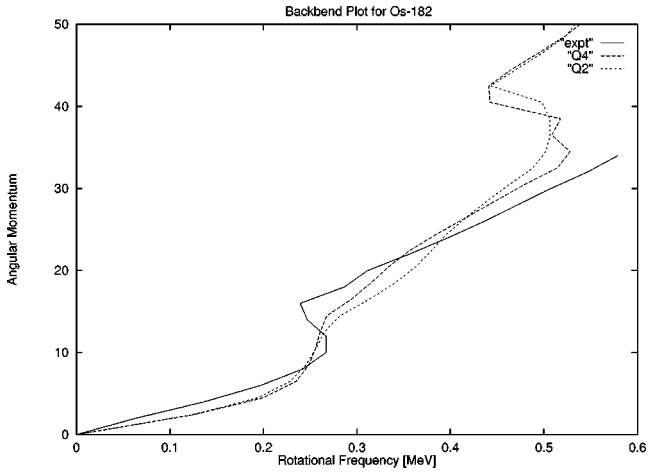

FIG. 1. Backbend plot for ^{182}Os showing the variation of angular momentum with rotational frequency ω. As indicated in the figure the solid line corresponds to the experimental data with $\omega_I = \frac{1}{2}(E_I - E_{I-2})$. The long-dashed curve, labeled ''Q4,'' corresponds to the case when both quadrupole and hexadecapole interaction terms are present in the Hamiltonian (1). The short-dashed curve, labeled ''Q2,'' indicates that only the quadrupole interaction is considered.

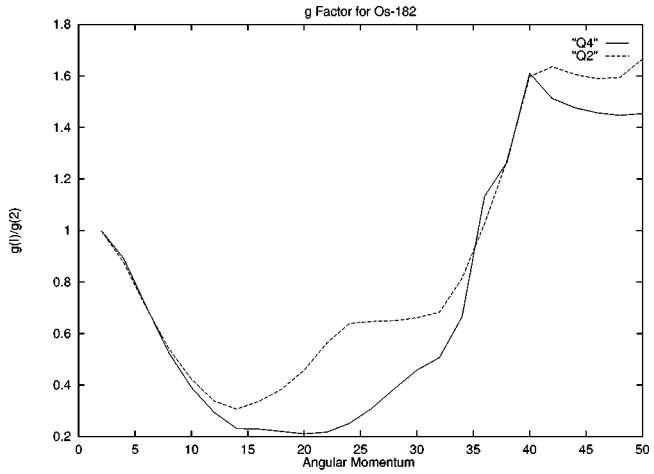

FIG. 3. Variation of the g factor ratio $g(I)/g(2)$ as a function of spin for both cases, that is, with the inclusion of the hexadecapole term (Q4) and without it (Q2).

next Fig. 2, where contributions from a few important orbitals to the total angular momentum are shown for the ''Q4'' case. At $I=14$ the contribution of $ni_{13/2}$ orbitals (mainly $m=7/2,9/2$ components) is about $9\hbar$, close to the experimental estimate of $10\hbar$ [8]. However, the alignment is not sudden enough around this spin to cause a sharp BB. Hence, we may conclude that some extra mechanism is, perhaps, needed to obtain a sharp first BB. We are trying to perform angular momentum projection, including K mixing, on CHFB wave functions. If this also fails, then, perhaps, a tilting mechanism is the only explanation.

However, the main interesting result here is the appearance of a second BB near $I=40$ as seen in Fig. 1. The small backward kink in the ''Q4'' curve at $I=36$ is a genuine one; that is, it is not due to some numerical inaccuracy, etc. The sharp BB is, of course, due to a sudden large and coherent alignment of the $pi_{13/2}$, $ph_{9/2}$, and $nj_{15/2}$ orbitals (mainly $m=1/2$ and 3/2 components) as clearly seen in Fig. 2. At $I=40$ the contribution of $ni_{13/2}$ suddenly drops by about six units in one step. The $nh_{9/2}$ orbitals contribute at all spins, in almost a gradual manner, whereas $ph_{11/2}$ orbitals start contributing at very high spins through high-m components. Thus, the structure near $I=40$ is very interesting. There is a quite sizable stretching of β, and γ acquires a negative value. That is, in this BB region, collectivity increases, rather than showing a decrease, as is often observed in the first band crossing region [19,20]. For the spin region $I=40$–50 the intrinsic structure remains essentially unchanged, which may be seen as a second minimum in a shell correction calculation, and levels for $I\geqslant40$ may be interpreted as rotational levels in the second well. The increase in β can be understood as due to an enhanced magnitude of the quadrupole matrix elements of the low-m, high-j (aligned) neutron and proton orbitals near the Fermi surface.

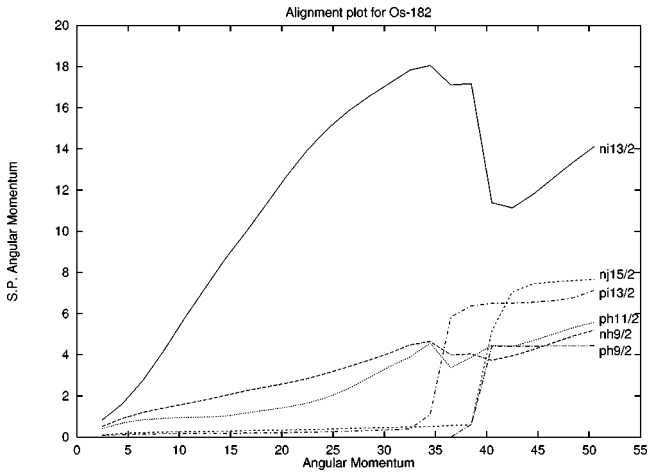

FIG. 2. Alignment plot. Contributions of a few important orbitals to the total spin are displayed denoted it as a single-particle (s.p.) contribution. These correspond to the ''Q4'' case only. The type of orbitals is indicated for each curve, where p and n indicate proton and neutron, respectively.

In Fig. 3 is displayed a variation of the g factors with spin. The actual value of $g(I=2)$ is 0.245 for the ''Q4'' case and 0.230 for the ''Q2'' case which appear to be reasonable in view of $g_R=0.27$ used in Ref. [8]. In both the cases the ratio $g(I)/g(2)$ drops sharply to a minimum at $I=14$, though in ''Q4'' case the real minimum is at $I=20$ with a slightly lower value. The sharp rise at $I=40$ is a clear indication of the large alignment of the proton orbitals. Beyond this the alignment of $nj_{15/2}$ orbitals stops the further rise. In the intermediate spin region ($I=20$–30) the relatively larger magnitude of the alignment of the large-m components of $ph_{11/2}$ make the g factors higher for the ''Q2'' case.

Finally we would like to make some additional remarks. Since at $I=40$ the pairing has collapsed in our calculation, one may think that in a particle-number-projected treatment the position of BB may get shifted or become much less dramatic. In order to check for this a calculation was performed for $I>30$ with a fixed value of Δ_p and Δ_n at about half of their values in the ground state. Then it is found that

γ changes sign between $I=32$ and 34 with all the characteristics as noted above. Thus, the second BB seen here seems very much genuine. We also notice a small favorable trend looking at the difference of the experimental γ-ray energies: $E_\gamma(32)-E_\gamma(30)=78$ keV and $E_\gamma(34)-E_\gamma(32)=65$ keV.

In conclusion, through a self-consistent CHFB calculation, which is very reliable at high spins, say, $I>20$, we have obtained a clear case of a sharp second backbend in ^{182}Os near $I=40$. This is caused by a large coherent alignment of low-m $pi_{13/2}$, $ph_{9/2}$, and $nj_{15/2}$ orbitals. In this spin region there is a substantial change of structure within a couple of units of angular momentum. For instance, γ goes positive to negative, with a change of 12° or more in one step, with an associated increase of β by about 20% (stretching). However, the first backbend is not well reproduced, and as discussed above, we are working on it. We have also studied the variation of g factors as a function of spin which essentially shows, in a gross manner, the alignment pattern of neutron and proton single-particle orbitals.

Particularly for ^{182}Os the levels are already known up to $I=34$; so we hope that our prediction will produce enough excitement in experimentalists to put efforts to study the interesting features in the spin $I=40$ region.

The author is grateful to Naoki Onishi for his kind support and many useful discussions. He would also like to acknowledge the financial support from the Japan Society for the Promotion of Science.

[1] B. Banerjee, H.-J. Mang, and P. Ring, Nucl. Phys. **A215**, 366 (1973).
[2] P. Ring and P. Schuck, *The Nuclear Many-Body Problem* (Springer-Verlag, New York, 1980).
[3] A. Faessler, M. Ploszajczak, and K. W. Schmid, Prog. Part. Nucl. Phys. **5**, 79 (1981).
[4] A. L. Goodman, Adv. Nucl. Phys. **11**, 263 (1979).
[5] A. Ansari and S. C. K. Nair, Nucl. Phys. **A283**, 326 (1977).
[6] A. Ansari, E. Wüst, and K. Mühlhans, Nucl. Phys. **A415**, 215 (1984).
[7] M. Diebel, A. N. Mantri, and U. Mosel, Nucl. Phys. **A345**, 72 (1980).
[8] T. Kutsarova *et al.*, Nucl. Phys. **A587**, 111 (1995).
[9] T. Shizuma, S. Mitarai, G. Sletten, R. A. Bark, N. L. Gjørup, H. J. Jensen, J. Wrzesinski, and M. Piiparinen, Nucl. Phys. **A593**, 247 (1995).
[10] C. S. Purry *et al.*, Nucl. Phys. **A632**, 229 (1998).
[11] P. M. Walker, G. D. Dracoulis, A. P. Byrne, B. Fabricius, T. Kibédi, A. E. Stuchbery, and N. Rowley, Nucl. Phys. **A568**, 397 (1994).
[12] C. J. Pearson *et al.*, Phys. Rev. Lett. **79**, 605 (1997).
[13] *Table of Isotopes*, 8th ed., edited by R. B. Firestone and V. S. Shirley (Wiley, New York, 1996).
[14] S. Frauendorf, Nucl. Phys. **A557**, 259c (1993).
[15] T. Horibata and N. Onishi, Nucl. Phys. **A596**, 251 (1996).
[16] M. Oi, N. Onishi, and T. Horibata, nucl-th/9806042.
[17] J. A. Sheikh, Y. Sun, and P. M. Walker, Phys. Rev. C **57**, R26 (1998).
[18] W. Nazarewicz, M. A. Riley, and J. D. Garrett, Nucl. Phys. **A512**, 61 (1990).
[19] M. Oshima, N. R. Johnson, F. K. McGowan, C. Baktash, I. Y. Lee, Y. Schutz, R. V. Ribas, and J. C. Wells, Phys. Rev. C **33**, 1988 (1986).
[20] M. N. Rao *et al.*, Phys. Rev. Lett. **57**, 667 (1986).